Heliyon 10 (2024) e30765

Contents lists available at ScienceDirect

Heliyon

journal homepage: www.cell.com/heliyon

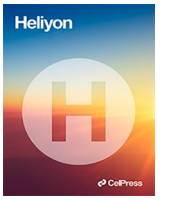

Research article

Enhancing catalytic activity of TiO_2 nanoparticles through acid treatment in Eosin-Y sensitized photohydrogen evolution reaction system

Jiwoo Shin [a,1], Jaeyoung Lee [a,b,1], Xiangyun Xiao [a,c], Taekyung Yu [a,*]

[a] *Department of Chemical Engineering, College of Engineering, Integrated Engineering Major, Kyung Hee University, Yongin, 17104, Republic of Korea*

[b] *School of Earth and Atmospheric Sciences, Georgia Institute of Technology, Atlanta, GA, 30332, United States*

[c] *Faculty of Materials Science and Engineering/Institute of Technology for Carbon Neutrality, Shenzhen Institute of Advanced Technology, Chinese Academy of Sciences, Shenzhen, 518055, PR China*

ARTICLE INFO

Keywords:
TiO_2 nanoparticle
Acid treatment
Photocatalytic hydrogen production
Electronic structure modification

ABSTRACT

Light-driven water splitting has gained increasing attention as an eco-friendly method for hydrogen production. There is a pressing need to enhance the performance of catalysts for the commercial viability of this reaction. Many methods have been proposed to improve catalyst performance; however, an economical and straightforward approach remains a priority. This paper presents an uncomplicated technique called acid treatment, which augments the catalytic performance of nanoparticles. The method promotes a change in the catalytic reactivity by causing a deficit in electron density of Ti and O on the surface of TiO_2 nanoparticles without altering their size, morphology, or crystal structure. In the Eosin Y sensitized photocatalytic hydrogen production system, nitric acid treated TiO_2 (16.95 μmol/g) exhibited 1.5 times the hydrogen production compared to bare TiO_2 (11.15 μmol/g).

Dear Dr. Christian Schulz.

1. Introduction

Harnessing solar energy and converting it into sustainable energy and fuel offers a viable solution to meet the growing global green energy needs and address the environmental challenges posed by burning fossil fuels. Photocatalysts, especially since Fujishima and Honda's initial use of TiO_2 in 1972, have emerged as promising tools for this purpose, drawing consistent attention from the green energy sector [1–5]. While TiO_2 boasts advantages such as earth abundance, nontoxicity, long-term stability, and affordability, its limited performance under visible light, owing to its considerable bandgap energy (~3.2 eV), curtails its broader applications [1,6–9]. In previous studies, emphasis was placed on doping TiO_2 materials with various atoms using diverse synthesis methods [10–12]. Presently, researchers are devoted to the advancement of photocatalyst fabrication through strategies such as dopant incorporation, leveraging crystal disorder induced by porosity, and doping with small atoms like hydrogen. Furthermore, novel synthesis methods are

* Corresponding author.
E-mail address: tkyu@khu.ac.kr (T. Yu).

[1] These authors contributed equally to this work.

https://doi.org/10.1016/j.heliyon.2024.e30765
Received 21 September 2023; Received in revised form 28 March 2024; Accepted 3 May 2024
Available online 7 May 2024

being employed to facilitate the doping of individual atoms onto the TiO_2 surface, aiming to maximize photocatalytic activity [13]. Consequently, there is an emphasis on devising a straightforward method to efficiently bolster catalyst activity, given the potential academic and industrial implications.

Catalytic reactions primarily transpire at the catalyst surface, emphasizing the importance of surface modifications in influencing reactivity. Therefore, various approaches have been explored to enhance catalytic activity by modifying the surface of the catalyst. While methods involving complex and precise multi-step processes to improve catalyst performance are promising, it is critically important to employ strategies that consider accessibility and ease of use in terms of scalability in research. In this aspect, acid treatment of the catalyst surface emerges as a prevalent and simple method to enhance its performance. Such treatments effectively remove surface impurities and modify key surface properties, like the metal oxidation state, reactive oxygen species, and defects [14–19]. The advantages of acid treatment extend beyond TiO_2, as it is actively researched for enhancing the photocatalytic performance of various catalyst materials such as $LaFeO_3$ [20], Co_3O_4 [21], $CuO–MoO_3/Al_2O_3$ [22], and others.

In this paper, we elucidate an easy-to-apply method to augment catalyst activity by modulating the electron density on the catalytic surface through acid treatment. We experimented with various laboratory acids to identify the optimal one for performance enhancement. Additionally, we analyzed the correlation between the acid quantity and activity. Our results indicate that, post acid treatment, hydrogen production in the Eosin Y sensitized photohydrogen system using TiO_2 surged by 1.52 times compared to its pretreatment levels.

2. Materials and methods

2.1. Materials

Hydrochloric acid (HCl, 37 %), nitric acid (HNO_3, 70 %), sulfuric acid (H_2SO_4, 99.999 %), titanium (IV) oxide (TiO_2, ≥99.5 %), and triethanolamine (TEOA, 99.0 %) were procured from Sigma Aldrich. Acid red 87 (Eosin Y, 90.0 %) was sourced from Tokyo Chemical Industry. All reagents were used as received without any further purification.

2.2. Acid treatment of TiO_2

Three acids (HNO_3, HCl, and H_2SO_4) were utilized to treat TiO_2. For each procedure, 0.51 mmol of TiO_2 was dispersed in 10 mL of

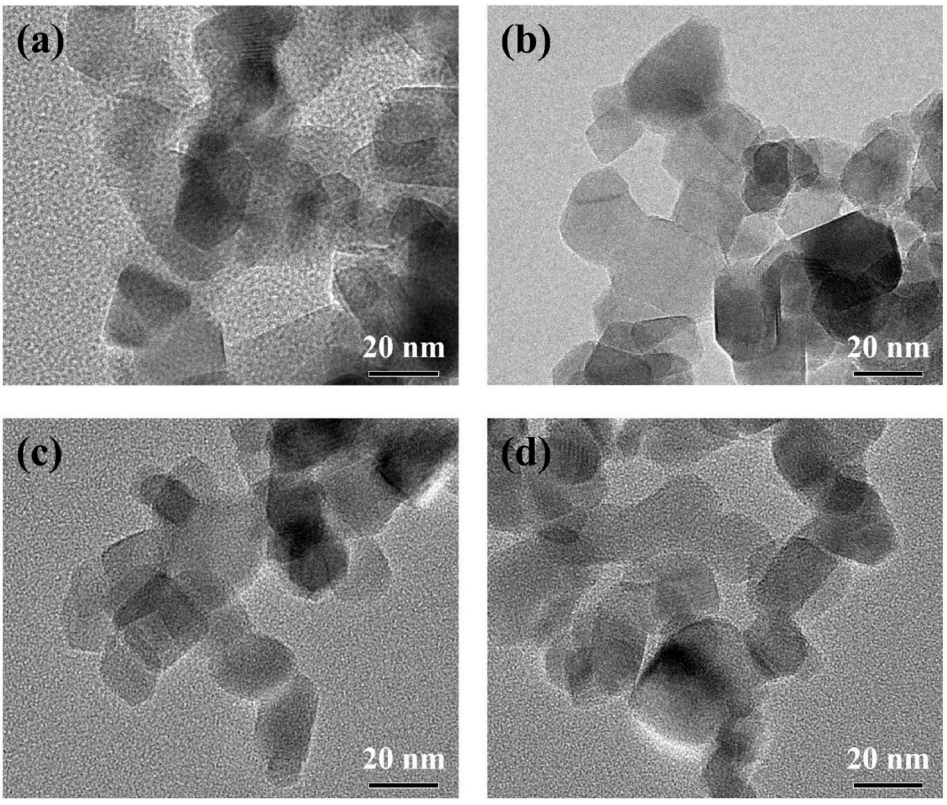

Fig. 1. Transmission electron microscopy images of TiO_2 nanoparticles subjected to different acid treatments. (a) Bare TiO_2, and (b) HNO_3, (c) HCl, (d) H_2SO_4 treated TiO_2.

deionized water. Given the varying concentrations of the acids, the requisite volume was precalculated to maintain consistency across the batches. This mixture was then subjected to magnetic stirring for 3 h in a 30 °C oil bath. Following this, it was washed with deionized water using centrifugation to ensure the complete removal of any residual acid. The treated TiO_2 samples were dried at room temperature overnight.

2.3. Characterization

Transmission electron microscopy (TEM) and high-resolution TEM (HRTEM) images were captured using a JEM-2100F (JEOL) at an operation of 200 keV. X-ray photoelectron spectroscopy (XPS) data, barring the 15 μL HNO_3 treated TiO_2 poststability test, was gathered using a NEXSA (Thermo Fisher Scientific) with monochromated, micro-focused, low power Al K-alpha X-ray source (wavelength: 0.83386 nm). In contrast, the 15 μL HNO_3 treated TiO_2, after the stability test, was analyzed using a PHI 5000 Versa Probe (ULVAC PHI) with monochromatized Al-Kα radiation. Powder X-ray diffraction (XRD) patterns were recorded using a MiniFlex 600 (Rigaku) with Cu-Kα radiation, scanning at a rate of 10°/min. Ultraviolet–visible diffusive reflectance spectroscopy (UV–vis DRS) data was obtained by using a spectrophotometer Cary 5000 (Varian) at 250–800 nm wavelength range (light source: Tungsten halogen visible and deuterium arc UV). Photoluminescence (PL) spectra data were obtained by using a fluorescence spectrometer FL6500 Luminescence system (PerkinElmer) using Xe lamp as light source.

2.4. Photocatalytic activity measurement

The photocatalytic hydrogen production procedure was conducted in a quartz reactor at room temperature, complemented by magnetic stirring. An aqueous solution, totaling 60 mL, was formulated by combining 3.18 mL of TEOA, 166.05 mg of Eosin Y, and 6 mg of the acid-treated TiO_2. This mixture was then transferred to a quartz reactor equipped with a magnetic stirrer, and the air within was purged using argon gas for 30 min. The reactor was positioned inside a light-obstructing box and illuminated using a 300 W Xe arc lamp (Newport 66902) that was equipped with an AM 1.5G filter, maintaining a stirring speed of 300 rpm. The volume of H_2 gas generated was gauged by extracting 0.1 mL of gas hourly, which was subsequently assessed through gas chromatography (YL6500 GC, Younglin, Korea).

3. Results and discussions

Fig. 1 illustrates the morphological evolution of TiO_2 after being treated with HNO_3, HCl, and H_2SO_4. The foundational material in this study is TiO_2, which also contains a modest rutile phase integrated within the anatase phase. Despite acid treatments, the morphology of TiO_2, having a diameter in the tens of nanometers range, remained largely unchanged (as seen in Fig. S1). To corroborate these findings, we gauged the lattice distances from HRTEM images. As a result, a consistent 3.4 Å spacing, corresponding to the (101) plane of anatase TiO_2, was prominently detected across all samples (Fig. S2) [23]. XRD patterns, before and after the acid treatment, displayed peaks that correlate with both anatase TiO_2 (JCPDS #21–1272) and rutile TiO_2 (JCPDS #21–1276). The absence of peak shifts affirms that the crystal structure remained unaltered post acid treatments (Fig. 2a) [24].

To delve into how the concentration of acid might influence the size and shape evolution of TiO_2, we modulated the HNO_3

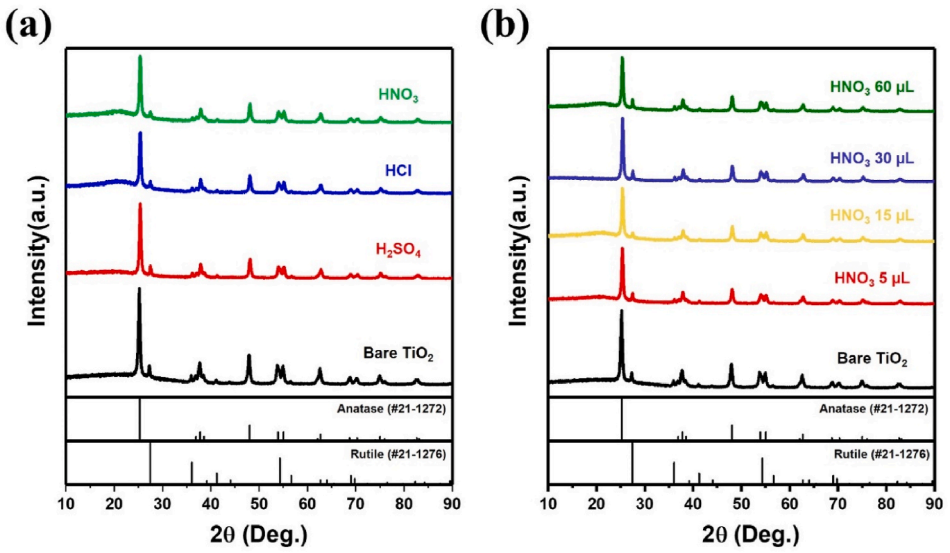

Fig. 2. XRD patterns of the TiO_2 nanoparticles treated with (a) various acids (HNO_3, HCl, and H_2SO_4) and (b) controlled amount of HNO_3 (5, 15, 30, 60 μL). References for anatase (JCPDS #21–1272) and rutile (JCPDS #21–1276) TiO_2 are provided for crystal structure comparison.

concentration during treatment. Interestingly, even with HNO_3 quantities ranging from 5 μL to 60 μL, the TEM images revealed persistent particle morphology (as depicted in Fig. S3). Using the same analytical approach previously adopted to understand TiO_2 differences by acid types, the lattice measurement of 3.4 Å that corresponded to the (101) plane of anatase TiO_2 remained consistent across all HRTEM images (Fig. S4). The XRD patterns further validated the HRTEM findings (Fig. 2b). Furthermore, the bandgap of the samples was determined via UV-DRS measurements. The results revealed slight differences, but no substantial deviation from the established bandgap of TiO_2 (~3.2 eV) (Fig. S5). Consequently, it can be concluded that neither the acid type nor the treatment amount influences the crystalline structure of TiO_2.

Nevertheless, while the crystalline structure was stable, the TiO_2 activity within the Eosin Y sensitized photocatalytic hydrogen production system exhibited variability based on the acid type and treatment volume (Fig. 4). To probe this discrepancy further, XPS analyses were performed to understand the microelectronic structure of TiO_2. Although the TEM images, XRD patterns, and DRS results showed consistency in TiO_2 nanoparticles both pre- and post-acid treatment, XPS data unveiled distinct surface variations. Specifically, Fig. 3a–d reveals the XPS peaks of Ti 2p and O 1s when TiO_2 underwent treatments with diverse acid types and concentrations. In Fig. 3a, the Ti 2p XPS peak bifurcated into Ti 2p3/2 and Ti 2p1/2. The binding energies for Ti 2p1/2 XPS peaks were

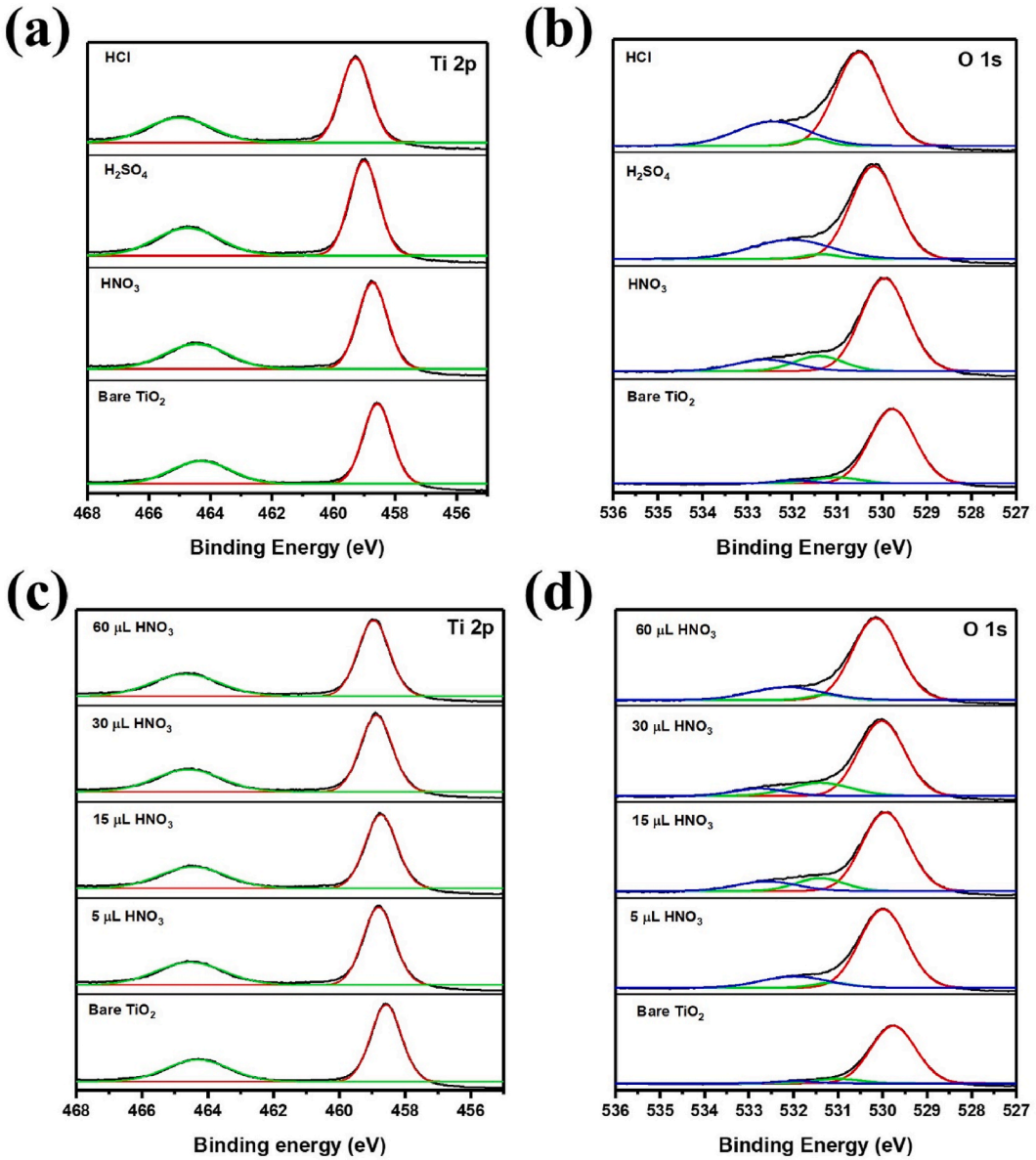

Fig. 3. X-ray photoelectron spectroscopy spectra of the TiO_2 nanoparticles. (a) Ti and (b) O spectra based on the type of acid treatment. (c) Ti and (d) O spectra corresponding to varying amounts of HNO_3 treatment (In b and d, red represents Ti–O, blue represents Ti–OH, and green represents oxygen vacancy).

systematically identified for bare TiO_2, HNO_3, H_2SO_4, and HCl treatments. This indicated a successive reduction in electron density in the sequence of HNO_3, H_2SO_4, and HCl. A similar pattern emerged in the XPS O 1s peak (Fig. 3b). Furthermore, in cases where TiO_2 was subjected to acid treatment, a consistent rise in the peak attributed to the hydroxyl group (blue) was noted. Specifically, in instances treated with nitric acid, there was a significant increase in the intensity of the peak associated with oxygen vacancies (green). Fig. 3c charts the XPS Ti 2p peaks as a function of varying HNO_3 volumes, with an overall increase in binding energy observed as HNO_3 volume amplified. This trend was also echoed in the XPS O 1s peaks (Fig. 3d). Additionally, the phenomenon of an increase in both the hydroxyl peak and oxygen vacancy peak was observed here as well after acid treatment. In particular, cases treated with 15 μL and 30 μL nitric acid exhibited a pronounced intensity of the oxygen vacancy peak. Hence, these evaluations corroborate that acid treatments indeed induce modifications in the microelectronic density of TiO_2.

We assessed the evolution of TiO_2's catalytic activity following acid treatment using the Eosin Y sensitized photocatalytic hydrogen production process. Fig. 4a and b present bar graphs that depict the volume of hydrogen produced over an hour, given a baseline condition of 60 mL total volume, 3.18 mL of TEOA, and 166.05 mg of Eosin Y. When juxtaposed with bare TiO_2 (11.15 μmol/g), TiO_2 exposed to 15 μL of HCl (13.44 μmol/g), H_2SO_4 (13.37 μmol/g), and HNO_3 (16.95 μmol/g) demonstrated enhanced hydrogen production by 20.52 %, 19.87 %, and 51.95 %, respectively (as shown in Fig. 4a). Further, when evaluating the activity with a gradual increment of HNO_3 from 5 μL to 60 μL, the peak value (16.95 μmol/g) was attained at 15 μL (Fig. 4b). From the combined insights of the photocatalytic and XPS analyses, we could infer that optimal photocatalytic activities might be achieved at a carefully calibrated

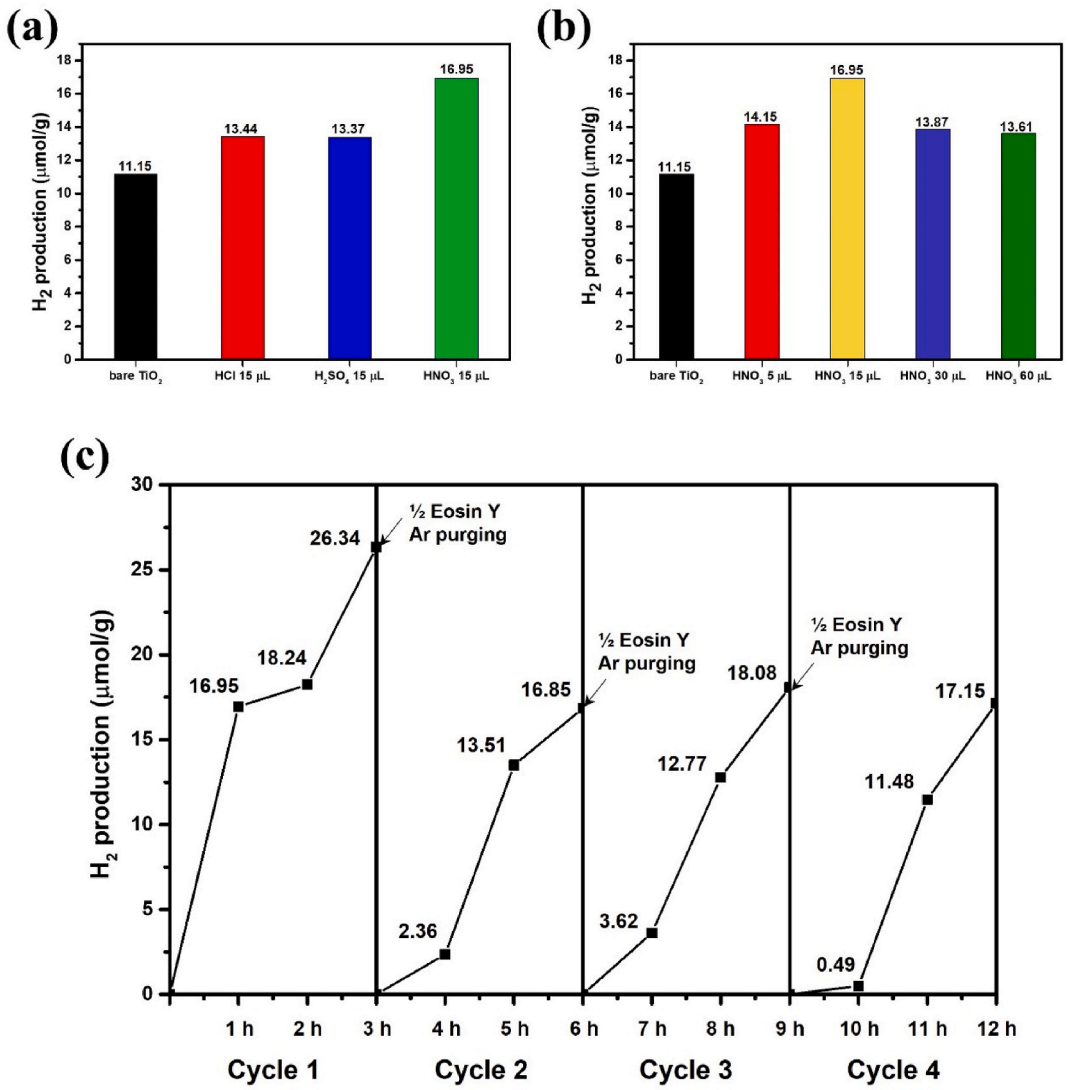

Fig. 4. Photocatalytic hydrogen production by TiO_2 nanoparticles. (a) Hydrogen production in 1 h based on the type of acid treatment (HCl, H_2SO_4, and HNO_3). (b) Hydrogen production in 1 h corresponding to varying amounts of HNO_3 treatment (5, 15, 30, and 60 μL). (c) Long-term (12 h) stability evaluation for TiO_2 treated with 15 μL of HNO_3.

electron density. This is underscored by the observation that a positive shift in binding energy and oxygen vacancy, representing reduced electron density, correlates positively with catalytic performance. Such phenomena might be attributed to surface anomalies like dangling bonds [25]. The surface of acid-treated TiO_2 manifests cation defects and oxygen vacancies leading to these dangling bonds. Such bonds can function as electron donors, fostering a synergistic effect that augments reactant adsorption [19,26]. Moreover, to investigate additional factors contributing to the enhancement of TiO_2 performance, we conducted PL emission spectrum measurements (Fig. S6). A notable observation from these findings is that acid-treated TiO_2 shows a lower intensity emission peak compared to bare TiO_2. Since efficient photocatalysis is known to be associated with a reduced degree of electron-hole recombination, these results serve as supporting evidence for the improved photocatalytic performance of acid-treated TiO_2.

The resilience of catalyst materials remains a critical factor of evaluation. Our investigation emphasized stability tests on samples treated with 15 μL of HNO_3. To gauge the reliability of TiO_2 treated with 15 μL of HNO_3, we conducted tests over four cycles (each cycle lasting 3 h). Between these cycles, Eosin Y was replenished, and argon purging was executed to facilitate error-free hydrogen production measurement. The inclusion of Eosin Y ensured the system's continuity, compensating for the Eosin Y used up in the photocatalytic process. Post the inaugural cycle's peak (26.34 μmol/g), the hydrogen volume produced in the subsequent cycle dipped by approximately 70 % (landing at 16.85 μmol/g). However, the third (18.08 μmol/g) and fourth cycles (17.15 μmol/g) evidenced a marginal uptick in hydrogen production compared to the second cycle. Besides, through a comparative analysis of the photocatalytic performance with diverse modifications applied to TiO_2 in relevant literature, we were able to assess the level of our results (Table S1). We further inspected the morphology and crystal structure of TiO_2 after a 12 h photocatalytic reaction (refer to Fig. S7). The TEM images indicated that the edges of the TiO_2 appeared somewhat blurred. However, the lattice spacing remained unchanged. The XRD pattern further affirmed the preservation of the innate crystal structure. Based on these observations, we deduce that TiO_2, when treated with HNO_3, retains its structural integrity and serves as a resilient catalyst even under prolonged reaction durations.

4. Conclusions

This research aimed to enhance the catalytic performance of TiO_2 using a straightforward acid treatment process. While treating TiO_2 with prevalent acids, including HCl, H_2SO_4, and HNO_3, we did not note any morphological or crystal structural changes. However, differences emerged in the Eosin Y sensitized photocatalytic hydrogen production when utilizing these treated materials as catalysts. XPS analysis highlighted that the surface electron density alterations and oxygen vacancy, resulting from acid treatment, played a pivotal role in catalytic reactivity. Our methodology underscores the potential of embracing simpler techniques alongside intricate methods to amplify the efficacy of existing catalyst activities. Combining this uncomplicated yet potent approach with intricate modification procedures can yield superior synergistic effects, paving the way for future research prospects.

CRediT authorship contribution statement

Jiwoo Shin: Writing – original draft, Software, Methodology, Investigation, Formal analysis, Data curation, Conceptualization. **Jaeyoung Lee:** Writing – original draft, Investigation, Formal analysis, Data curation. **Xiangyun Xiao:** Investigation, Formal analysis. **Taekyung Yu:** Writing – review & editing, Supervision, Resources, Project administration, Funding acquisition, Conceptualization.

Declaration of competing interest

The authors declare that they have no known competing financial interests or personal relationships that could have appeared to influence the work reported in this paper.

Acknowledgments

This research received financial support from the National Research Foundation of Korea (NRF) through the grants NRF-2022M3H4A7046278 and 2020R1A2C1003885. Additional backing came from the Korea Institute for Advancement of Technology and the Ministry of Trade, Industry & Energy of the Republic of Korea, under the grant number P0017363.

Appendix A. Supplementary data

Supplementary data to this article can be found online at https://doi.org/10.1016/j.heliyon.2024.e30765.

References

[1] H. Eidsvåg, S. Bentouba, P. Vajeeston, S. Yohi, D. Velauthapillai, TiO_2 as a photocatalyst for water splitting-an experimental and theoretical review, Molecules 26 (2021) 1687.
[2] M. Ijaz, M. Zafar, Titanium dioxide nanostructures as efficient photocatalyst: progress, challenges and perspective, Int. J. Energy Res. 45 (2021) 3569–3589.
[3] J. Cai, J. Shen, X. Zhang, Y.H. Ng, J. Huang, W. Guo, C. Lin, Y. Lai, Light-driven sustainable hydrogen production utilizing TiO_2 nanostructures: a review, Small Methods 3 (2019) 1800184.
[4] A.L. Linsebigler, G. Lu, J.T. Yates, Photocatalysis on TiO_2 surfaces: principles, mechanisms, and selected results, Chem. Rev. 95 (1995) 735–758.

[5] R. Asahi, T. Morikawa, T. Ohwaki, K. Aoki, Y. Taga, Visible-light photocatalysis in nitrogen-doped titanium oxides, Science 293 (5528) (2001) 269–271.
[6] M. Kapilashrami, Y. Zhang, Y.S. Liu, A. Hagfeldt, J. Guo, Probing the optical property and electronic structure of TiO_2 nanomaterials for renewable energy applications, Chem. Rev. 114 (2014) 9662–9707.
[7] D.O. Scanlon, C.W. Dunnill, J. Buckeridge, S.A. Shevlin, A.J. Logsdail, S.M. Woodley, C.R. Catlow, M.J. Powell, R.G. Palgrave, I.P. Parkin, G.W. Watson, T. W. Keal, P. Sherwood, A. Walsh, A.A. Sokol, Band alignment of rutile and anatase TiO_2, Nat. Mater. 12 (2013) 798–801.
[8] M.R. Hoffmann, S.T. Martin, W. Choi, D.W. Bahnemann, Environmental applications of semiconductor photocatalysis, Chem. Rev. 95 (1995) 69–96.
[9] S.U.M. Khan, M. Al-Shahry, W.B. Ingler, Efficient photochemical water splitting by a chemically modified n-TiO_2, Science 297 (5590) (2002) 2243–2245.
[10] S. Al Jitan, G. Palmisano, C. Garlisi, Synthesis and surface modification of TiO2-based photocatalysts for the conversion of CO_2, Catalysts 10 (2020) 227.
[11] V. Kumaravel, S. Mathew, J. Bartlett, S.C. Pillai, Photocatalytic hydrogen production using metal doped TiO_2: a review of recent advances, Appl. Catal. B Environ. 244 (2019) 1021–1064.
[12] J. Nowotny, M.A. Alim, T. Bak, M.A. Idris, M. Ionescu, K. Prince, M.Z. Sahdan, K. Sopian, M.A. Mat Teridi, W. Sigmund, Defect chemistry and defect engineering of TiO_2-based semiconductors for solar energy conversion, Chem. Soc. Rev. 44 (2015) 8424–8442.
[13] J.-P. Jeon, D.H. Kweon, B.J. Jang, M.J. Ju, J.-B. Baek, Enhancing the photocatalytic activity of TiO_2 catalysts, Adv. Sustainable Syst. 4 (2020) 2000197.
[14] J.C. Yu, J. Yu, J. Zhao, Enhanced photocatalytic activity of mesoporous and ordinary TiO_2 thin films by sulfuric acid treatment, Appl. Catal. B Environ. 36 (2002) 31–43.
[15] X. Yang, X. Yu, M. Lin, X. Ma, M. Ge, Enhancement effect of acid treatment on Mn_2O_3 catalyst for toluene oxidation, Catal. Today 327 (2019) 254–261.
[16] W. Si, Y. Wang, Y. Peng, X. Li, K. Li, J. Li, A high-efficiency gamma-MnO_2-like catalyst in toluene combustion, Chem. Commun. 51 (2015) 14977–14980.
[17] J.-H. Lee, R. Black, G. Popov, E. Pomerantseva, F. Nan, G.A. Botton, L.F. Nazar, The role of vacancies and defects in $Na_{0.44}MnO_2$ nanowire catalysts for lithium–oxygen batteries, Energy Environ. Sci. 5 (2012) 9558.
[18] J. Quiroz, J.-M. Giraudon, A. Gervasini, C. Dujardin, C. Lancelot, M. Trentesaux, J.-F. Lamonier, Total oxidation of formaldehyde over MnO_x-CeO_2 catalysts: the effect of acid treatment, ACS Catal. 5 (2015) 2260–2269.
[19] W. Si, Y. Wang, S. Zhao, F. Hu, J. Li, A facile method for in situ preparation of the MnO_2/$LaMnO_3$ catalyst for the removal of toluene, Environ. Sci. Technol. 50 (2016) 4572–4578.
[20] Q. Yang, J. Li, D. Wang, Y. Peng, Y. Ma, Activity improvement of acid treatment on $LaFeO_3$ catalyst for CO oxidation, Catal. Today 376 (2021) 205–210.
[21] G. Li, C. Zhang, Z. Wang, H. Huang, H. Peng, X. Li, Fabrication of mesoporous Co_3O_4 oxides by acid treatment and their catalytic performances for toluene oxidation, Appl. Catal. Gen. 550 (2018) 67–76.
[22] C.-H. Wang, C.-N. Lee, H.-S. Wang, Effect of acid treatment on the performance of the CuO- MoO_3/Al_2O_3 catalyst for the destructive oxidation of $(CH_3)_2S_2$, Ind. Eng. Chem. Res. 37 (1998) 1774–1780.
[23] K. Sakurai, M. Mizusawa, X-ray diffraction imaging of anatase and rutile, Anal. Chem. 82 (2010) 3519–3522.
[24] J. Wang, J. Yu, X. Zhu, X.Z. Kong, Preparation of hollow TiO_2 nanoparticles through TiO_2 deposition on polystyrene latex particles and characterizations of their structure and photocatalytic activity, Nanoscale Res. Lett. 7 (2012) 646.
[25] Z. Li, X. Wang, M. Zeng, K. Chen, D. Cao, Y. Huang, Y. Zhu, W. Zhang, N. Wang, Y.A. Wu, The interplay between selective etching induced cation defects and active oxygen species for volatile organic compounds degradation, J. Colloid Interface Sci. 625 (2022) 363–372.
[26] D.C. Moritz, W. Calvet, M.A. Zare Pour, A. Paszuk, T. Mayer, T. Hannappel, J.P. Hofmann, W. Jaegermann, Dangling bond defects on si surfaces and their consequences on energy band diagrams: From a photoelectrochemical perspective, Sol. RRL 7 (2023) 2201063.